

FABRICATION AND MECHANICAL PROPERTIES OF HYALURONIC ACID MICRONEEDLE
ARRAYS FOR TRANSDERMAL DRUG DELIVERY



A Thesis Submitted in Partial Fulfillment of the Requirements
for the Degree of Master of Science in Chemistry
Department of Chemistry
Faculty of Science
Chulalongkorn University
Academic Year 2018
Copyright of Chulalongkorn University

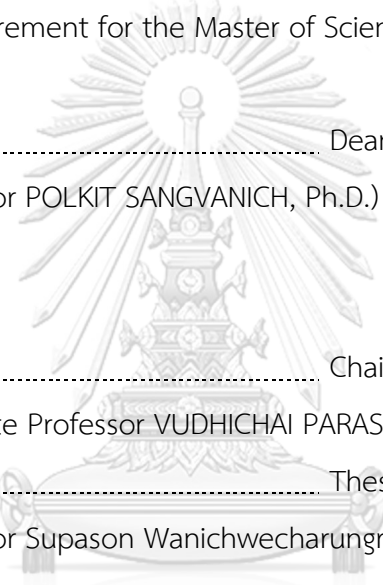
การสร้างและสมบัติเชิงกลของแอร์เรย์เซมิคอนดักเตอร์ระดับไมครอนประเภทกรตไฮยาโลโรนิกสำหรับการ
นำส่งยาผ่านผิวหนัง



วิทยานิพนธ์นี้เป็นส่วนหนึ่งของการศึกษาตามหลักสูตรปริญญาวิทยาศาสตรมหาบัณฑิต
สาขาวิชาเคมี ภาควิชาเคมี
คณะวิทยาศาสตร์ จุฬาลงกรณ์มหาวิทยาลัย
ปีการศึกษา 2561
ลิขสิทธิ์ของจุฬาลงกรณ์มหาวิทยาลัย

Thesis Title	FABRICATION AND MECHANICAL PROPERTIES OF HYALURONIC ACID MICRONEEDLE ARRAYS FOR TRANSDERMAL DRUG DELIVERY
By	Mr. Teeranut Rutwaree
Field of Study	Chemistry
Thesis Advisor	Professor Supason Wanichwecharungruang, Ph.D.

Accepted by the Faculty of Science, Chulalongkorn University in Partial
Fulfillment of the Requirement for the Master of Science



..... Dean of the Faculty of Science
(Professor POLKIT SANGVANICH, Ph.D.)

THESIS COMMITTEE

..... Chairman
(Associate Professor VUDHICHAIR PARASUK, Ph.D.)

..... Thesis Advisor
(Professor Supason Wanichwecharungruang, Ph.D.)

..... Examiner
(Assistant Professor ROJRIT ROJANATHANES, Ph.D.)

..... External Examiner
(Professor Tawan Sooknoi, Ph.D.)

ธีรณัฐ รุทธีวารี : การสร้างและสมบัติเชิงกลของแออร์เรย์เข็มฉีดยาระดับไมครอนประเภท
กรดไฮยาลูโรนิกสำหรับการนำส่งยาผ่านผิวหนัง. (FABRICATION AND MECHANICAL
PROPERTIES OF HYALURONIC ACID MICRONEEDLE ARRAYS FOR
TRANSDERMAL DRUG DELIVERY) อ.ที่ปรึกษาหลัก : ศ. ดร.ศุภศร วนิชเวหารุ่งเรือง

เข็มฉีดยาระดับไมครอนประเภทละลายน้ำได้ได้รับความสนใจอย่างแพร่หลายเพื่อเป็น
ทางเลือกแทนเข็มฉีดยาหรือระบบนำส่งยาอื่นๆ พอลิเมอร์หลายชนิดถูกนำมาผลิตเป็นเข็มฉีดยา
ระดับไมครอน ชนิดของพอลิเมอร์ส่งผลต่อสมบัติเชิงกลและอัตราการละลายของเข็มฉีดยาระดับ
ไมครอน ในงานวิจัยนี้ได้สังเคราะห์เข็มฉีดยาระดับไมครอนจากพอลิเมอร์ผสมกรดไฮยาลูโรนิกและ
พอลิไวนิลไพโรลิโดนที่ 5 สัดส่วน (กรดไฮยาลูโรนิก/พอลิไวนิลไพโรลิโดนที่ 100/0, 75/25, 50/50,
25/50, 0/100) และแออร์เรย์เข็มฉีดยาระดับไมครอนจากกรดไฮยาลูโรนิกที่ผ่านการเชื่อมโยง
ระหว่างโมเลกุล (crosslinking) สมบัติเชิงกลของเข็มฉีดยาระดับไมครอนที่สังเคราะห์ขึ้นได้
วิเคราะห์ด้วยเครื่องวัดแรงดึงแรงอัดและเครื่องวัดความแข็ง ความสามารถในการกักตุนและอัตรา
การละลายของแออร์เรย์เข็มฉีดยาระดับไมครอนก็ถูกทดสอบโดยใช้หนังหมู ผลการทดลองแสดงว่า
เข็มฉีดยาระดับไมครอนที่มีสัดส่วนของพอลิไวนิลไพโรลิโดนสูงจะมีสมบัติเชิงกลที่ดีกว่าและมีอัตรา
การละลายที่เร็วกว่า โดยเข็มฉีดยาระดับไมครอนผลิตจากกรดไฮยาลูโรนิก/พอลิไวนิลไพโรลิโดนที่
สัดส่วน 50/50 กรดไฮยาลูโรนิก/พอลิไวนิลไพโรลิโดนที่สัดส่วน 25/50 และ พอลิไวนิลไพโรลิโดน
เท่านั้นที่สามารถแทงทะลุผ่านหนังหมูได้

จุฬาลงกรณ์มหาวิทยาลัย
CHULALONGKORN UNIVERSITY

สาขาวิชา เคมี
ปีการศึกษา 2561

ลายมือชื่อนิสิต
ลายมือชื่อ อ.ที่ปรึกษาหลัก

5971982123 : MAJOR CHEMISTRY

KEYWORD: dissolvable microneedle, Mechanical property, dissolution rate

Teeranut Rutwaree : FABRICATION AND MECHANICAL PROPERTIES OF
HYALURONIC ACID MICRONEEDLE ARRAYS FOR TRANSDERMAL DRUG
DELIVERY. Advisor: Prof. Supason Wanichwecharungruang, Ph.D.

Dissolvable microneedles have been widely investigated as an alternative of hypodermic injection or other drug delivery methods. Various polymers have been used to fabricate microneedles. Type of polymers affects mechanical properties and dissolution rate of microneedles. In this study, five formulations of hyaluronic acid (HA)/ polyvinylpyrrolidone (PVP) composite microneedle patches (HA/PVP at 100/0, 75/25, 50/50, 25/50, 0/100) were fabricated. The crosslinked HA microneedles were also fabricated. Mechanical properties of the obtained microneedles were determined by universal testing machine and durometer. The skin-penetration ability and dissolution rate of HA/PVP microneedles were also investigated using porcine skin. The results show that microneedle patches with higher PVP content possessed a higher compressive strength and dissolution rate and only the microneedle patches made of 50/50 HA/PVP, 25/75 HA/PVP, and PVP could penetrate the skin.

จุฬาลงกรณ์มหาวิทยาลัย
CHULALONGKORN UNIVERSITY

Field of Study: Chemistry

Student's Signature

Academic Year: 2018

Advisor's Signature

ACKNOWLEDGEMENTS

Firstly, I would like to express my sincere appreciation and gratitude to my advisor Prof. Supason Wanichwecharungruang for the continuous support of my Master degree study and related research, for her patience, motivation, and immense knowledge throughout this work.

I am sincerely grateful to the members of the thesis committee, Assoc. Prof. Vudhichai Parasuk, Asst. Prof. Rojrit Rojanathanes, Prof. Tawan Sooknoi for their valuable comments and suggestion.

I would like to thank my members of the SW research group for the good working environment, for their support, encouragement, and advice.

And I gratefully acknowledge the scholarship from the graduate school, Chulalongkorn University to commemorate the 72nd anniversary of his Majesty King Bhumibol Aduladej.

Finally, I would like to thank and take this opportunity to express my sincere appreciation to my parents for their encouragement, activation, and support throughout the entire research study. This accomplishment would not have been possible without them.



จุฬาลงกรณ์มหาวิทยาลัย
CHULALONGKORN UNIVERSITY

Teeranut Rutwaree

TABLE OF CONTENTS

	Page
.....	iii
ABSTRACT (THAI).....	iii
.....	iv
ABSTRACT (ENGLISH).....	iv
ACKNOWLEDGEMENTS.....	v
TABLE OF CONTENTS.....	vi
List of Table.....	vii
List of Figure.....	viii
CHAPTER I INTRODUCTION.....	1
1.1 Introduction.....	1
1.2 Literature reviews.....	2
1.2.1 Fabrication technique.....	2
1.2.1.1 Preparing molds for fabricate microneedles patch.....	3
1.2.1.2 Casting the polymer into the mold.....	3
1.2.1.3 Solidifying by drying or crosslinking.....	3
1.2.1.4 Removing microneedles from the mold.....	3
1.2.2 Material for fabricate microneedles patch.....	3
1.2.2.1 HA microneedles patches.....	3
1.2.2.2 PVP microneedles patches.....	6
1.2.2.3 PVP-PVA microneedles patches.....	6
CHAPTER II EXPERIMENTAL.....	8

2.1 Materials and chemicals	8
2.2 Instruments and equipment	8
2.3 Fabrication of HA/PVP microneedle patches	9
2.5 Synthesis and characterization of acrylate modified HA	9
2.6 Fabrication of crosslinked-HA-microneedle patches	10
2.7 Mechanical testing of HA/PVP microneedle patches	11
2.8 <i>Ex vivo</i> skin penetration test of HA/PVP microneedle patches.....	11
2.9 <i>In situ</i> dissolution rate of microneedle in porcine ear skin.....	12
2.10 Fabrication of retinal loaded HA/PVP microneedle patches	12
CHAPTER III RESULTS AND DISCUSSIONS	14
3.1 Fabrication of HA/PVP microneedle patches	14
3.2 Synthesis and characterization of acrylate modified HA (m-HA).....	15
3.3 Fabrication of crosslinked-HA-microneedle patches	17
3.4 Mechanical testing of HA/PVP microneedle patches	21
3.5 <i>Ex vivo</i> skin penetration test of HA/PVP microneedle patches.....	27
3.6 <i>In situ</i> dissolution rate of microneedle in porcine ear skin.....	28
3.7 Fabrication of retinal-loaded HA/PVP microneedle patches	30
CHAPER IV CONCLUSION	33
REFERENCES	34
VITA.....	36

List of Table

Table 2. 1 The amount of polymer for the preparation of HA/PVP solution	9
Table 2. 2 The amount of reagents for the preparation of m-HA solution.....	10
Table 3. 1 Appearance of the products formed under different Crosslinking conditions	19
Table 3. 2 Shore A hardness of different polymer films and skin	26



List of Figure

Figure 1. 1 Schematic illustration of process for fabricating microneedles patch ²	2
Figure 1. 2 Schematic of the HA crosslinking reaction via radical polymerization reaction	5
Figure 1. 3 Characterization of the HA microneedles patches. Schematic of the fabrication process of microneedles patch (A), photograph of the microneedles patch (B), fluorescence microscopy image of fluorescein-labeled insulin loaded microneedles patch (C), SEM image of microneedles patch (D), mechanical characteristic of non-crosslinked and crosslinked microneedles patches. ⁵	5
Figure 1. 4 <i>In vitro</i> skin insertion capability of Lissamine green B loaded PVP microneedles patch. Stereomicroscopy images of microneedles before insertion (A1), after insertion (A2). Porcine skin after the insertion of Lissamine green B loaded PVP microneedles patch (A3-A4)	6
Figure 1. 5 <i>In vitro</i> drug-release profiles of fluorescein-labeled bovine serum albumin loaded PVP-PVA = 1:1 and PVP-PVA = 1:4 microneedles patch ⁴	7
Figure 2. 1 Schematic setup of compression test of HA/PVP microneedle performed by UTM.....	11
Figure 2. 2 Schematic of <i>in situ</i> dissolution rate of microneedle in porcine ear skin testing	12
Figure 3. 1 Stereomicroscopic and SEM images of HA/PVP microneedle patches made of (A) HA, (B) HA/PVP at 75/25, (C) HA/PVP at 50/50, (D) HA/PVP at 25/75, (E) PVP.....	14
Figure 3. 2 The mechanism of m-HA <i>via</i> esterification reaction.	15
Figure 3. 3 ¹ H NMR spectra of HA, and m-HA in D ₂ O.....	16
Figure 3. 4 The mechanism of crosslinked m-HA <i>via</i> esterification reaction.....	18
Figure 3. 5 The image of m-HA microneedle patches fabricated under difference conditions as shown in table 1.1.....	19

Figure 3. 6 Stereomicroscopic image of crosslinked-HA-microneedle patches.	20
Figure 3. 7 Mechanical characteristic of HA microneedle patch.....	21
Figure 3. 8 Stereomicroscopic images of HA microneedle patch (A) before and (B) after the compressive test. SEM image of the HA microneedle patch after the compressive test is shown in (C).	21
Figure 3. 9 Mechanical characteristic of HA/PVP at 75/25 microneedle patch.....	22
Figure 3. 10 Stereomicroscopic images of 75/25 HA/PVP microneedle patch (A) before and (B) after the compressive test. SEM image of the 75/25 HA/PVP microneedle patch after the compressive test (C).	22
Figure 3. 11 Mechanical characteristic of HA/PVP at 50/50 microneedle patch.....	23
Figure 3. 12 Stereomicroscopic images of 50/50 HA/PVP microneedle patch (A) before and (B) after the compressive test. SEM image of the 50/50 HA/PVP microneedle patch after the compressive test (C).	23
Figure 3. 13 Mechanical characteristic of HA/PVP at 25/75 microneedle patch.....	24
Figure 3. 14 Stereomicroscopic images of 25/75 HA/PVP microneedle patch (A) before and (B) after the compressive test. SEM image of the 25/75 HA/PVP microneedle patch after the compressive test (C).	24
Figure 3. 15 Mechanical characteristic of PVP microneedle patch.	25
Figure 3. 16 Stereomicroscopic images of PVP microneedle patch (A) before and (B) after the compressive test. SEM image of the PVP microneedle patch after the compressive test (C).	25
Figure 3. 17 Mechanical characteristic of different microneedle patches: HA (blue), 75/25 HA/PVP (yellow), 50/50 HA/PVP (red), 25/75 HA/PVP (black), and PVP (green)...	26
Figure 3. 18 Top view of the <i>ex vivo</i> skin that had been treated with of microneedle patches made of (A) HA, (B) 75/25 HA/PVP, (C) 50/50 HA/PVP, (D) 25/75 HA/PVP, and (E) PVP.....	27

- Figure 3. 19** The top view picture of porcine ear skin that had been treated with 50/50 HA/PVP microneedle patch and was submerged in release medium. Each picture shows the top view of the skin at various times post application. 28
- Figure 3. 20** The top view picture of porcine ear skin that had been treated with 25/75 HA/PVP microneedle patch and was submerged in release medium. Each picture shows the top view of the skin at various times post application. 29
- Figure 3. 21** The top view picture of porcine ear skin that had been treated with PVP microneedle patch and was submerged in release medium. Each picture shows the top view of the skin at various times post application. 29
- Figure 3. 22** Relationship between % different gray value between black dot array and surrounding area and time of 50/50 HA/PVP (red), 25/75 HA/PVP (black), and PVP (green) microneedle patches..... 30
- Figure 3. 23** Stereomicroscopic image of retinal-loaded HA/PVP microneedle patches (A) SEM image of retinal loaded HA/PVP microneedle patch (B-C). 31
- Figure 3. 24** Mechanical characteristic of 50/50 HA/PVP microneedle patches (red), retinal-loaded HA/PVP microneedle patches (purple). 31
- Figure 3. 25** Stereomicroscopic images of retinal loaded microneedle patch (A) after compressive test (B). 31
- Figure 3. 26** Mechanical characteristic at the low displacement of 50/50 HA/PVP microneedle patches (red), retinal-loaded HA/PVP microneedle patches (purple). 32

CHAPTER I

INTRODUCTION

1.1 Introduction

Transdermal delivery is an attractive alternative to oral delivery of drugs and hypodermic injection. It has several advantages compared to the oral route. It can bypass hepatic first pass effect which may prematurely metabolize drugs. Transdermal delivery also has advantages over hypodermic injections. It is not painful, so it can improve patient compliance.¹⁻³ Unfortunately, only low molecular drugs (<600 Da) can be passively delivered into the skin across the stratum corneum, the outer most layer of the skin.²

Recently, dissolvable microneedles have received considerable attention because it has advantages over other delivery systems. It is able to deliver a wide range of therapeutics, easy to use and inexpensive. The dissolvable microneedles also does not leave needles waste, thus lower the risk of the disease transmission by re-use of the needle.³ Drug can be incorporated into the needles and deposited into skin. Length and shape of the needles can be designed to fit the purposes easily. Usually, dissolvable microneedles with the needles height of less than 1000 μm can deliver drugs without stimulating nerves and damaging blood vessels.^{2,4} Dissolvable microneedles are usually made of biodegradable and biocompatible polymers such as hyaluronic acid (HA),⁵⁻⁷ carboxymethylcellulose (CMC),⁸ polyvinyl alcohol (PVA),^{9, 10} and polyvinylpyrrolidone (PVP).¹¹⁻¹³ The difference polymers would affect mechanical properties of the needles and the dissolution rate of microneedles. HA is one of the most popular polymers for fabricating microneedles. It is a natural water-soluble polymer that can be found in all tissues and many body fluids. It is widely used as a cosmetic ingredient and an injectable cosmetic filler.⁶ However, HA has poor mechanical properties. In order to improve the mechanical properties, it is necessary to crosslink the HA. However,

crosslinked HA will take a longer time to dissolve, so it possesses higher risks of clogging capillary and rejection by the body, when compared to non-crosslinked HA. Crosslinked-HA-microneedles also need to be pressed on the skin for a long time to wait until it dissolves. This can cause the uncomfortable feeling and skin irritation.¹⁴ PVP has also been used for fabricating microneedles. It can be fabricated without crosslinking.¹¹⁻¹³ It possesses a rapid dissolution rate.

Here, we report our studies on the use of HA and PVP at various ratios to make microneedles. We also study the mechanical properties, the dissolution rate, and the skin penetration ability (using *ex vivo* porcine skin) of the microneedle patches prepared through different formulation.

1.2 Literature reviews

1.2.1 Fabrication technique

There are various methods for fabricating dissolvable microneedle patch such as droplet-borne air blowing (DAB),¹⁵ drawing lithography,¹⁶ and micromolding.⁵⁻¹⁰ Micromolding is the most popular. There are four main steps to fabricate microneedles with this method (Figure 1.1).

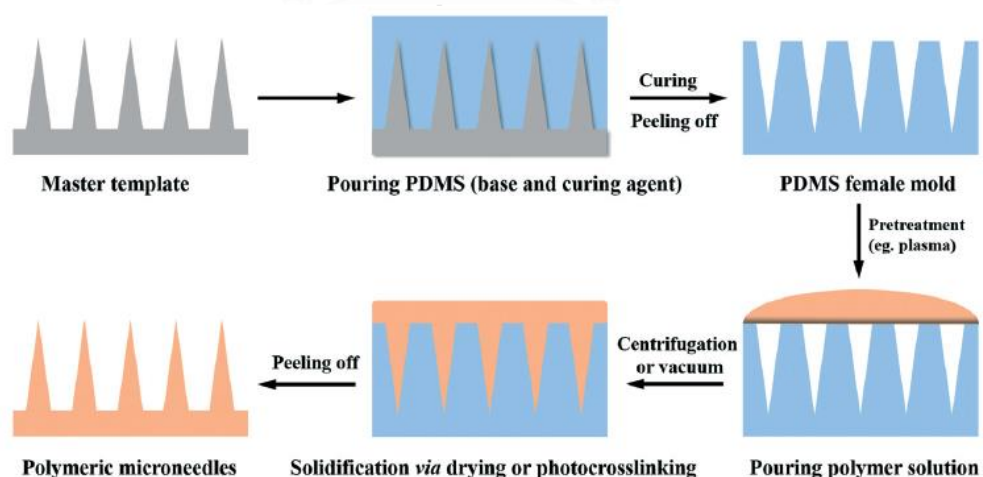


Figure 1. 1 Schematic illustration of process for fabricating microneedles patch²

1.2.1.1 Preparing molds for fabricate microneedles patch

The microneedle mold can be made from several materials such as ceramics,⁹ PVA,¹⁷ polydimethylsiloxane (PDMS).^{4, 6} PDMS is the most widely used because it has good durability, and poor adhesion. With its poor adhesion, it is easy to separate the microneedles from the mold. More importantly, it is easy to replicate the PDMS mold shape from the master template (Figure 1.1).

1.2.1.2 Casting the polymer into the mold

The PDMS has hydrophobic surface. Thus, the hydrophilic polymer solution cannot fill the mold easily due to the small needle volume. To overcome this problem, the centrifugation is popularly used to force the polymer to fill the mold (Figure 1.1).

1.2.1.3 Solidifying by drying or crosslinking

After filling the polymer solution into the mold, it was left to dry in order to solidify the microneedles. The polymer with poor mechanical strength may need to be crosslinked in this step to achieve a better strength.

1.2.1.4 Removing microneedles from the mold

The polymer that is completely dry could be removed from the PDMS mold easily without damaging the needles due to the hydrophobic surface of the PDMS mold. The shape of the microneedles resembles the mold shape.

1.2.2 Material for fabricate microneedles patch

There are various polymers to fabricate microneedles such as hyaluronic acid (HA),⁵⁻⁷ carboxymethylcellulose (CMC),⁸ polyvinyl alcohol (PVA),^{9, 10} and polyvinylpyrrolidone (PVP).¹¹⁻¹³

1.2.2.1 HA microneedles patches

HA is a biocompatible water-soluble polysaccharide composed of repeated units of β -1,4-D-glucuronic acid and β -1,3-N-acetyl-D-glucosamine. It can be

found abundantly in all tissues and body fluids, especially in the skin. It is widely used as a cosmetic ingredient and an injectable cosmetic filler for soft tissue augmentation. With its high biocompatibility, HA is an excellent material for fabricate dissolvable microneedles patches.⁶

In 2015, Yu and co-worker fabricated dissolvable microneedles patches from HA for insulin delivery. To improve the mechanical properties of the needles, they crosslinked the HA by introducing double bonds in the HA chains and running the radical polymerization reaction (**Figure 1.2**). They successfully fabricated the conical shape microneedles using micromolding method with centrifugation (**Figure 1.3 A-D**). They measured the mechanical strength using tensile compression machine comparing non-crosslinked microneedles with crosslinked microneedles. The result shows that crosslinked microneedle has failure force of 0.06 N per needle, while non-crosslinked microneedles has failure force of 0.02 N per needle (**Figure 1.3 E**). They also found that the stiffness of crosslinked MNs provided sufficient strength to penetrate skin without breaking.

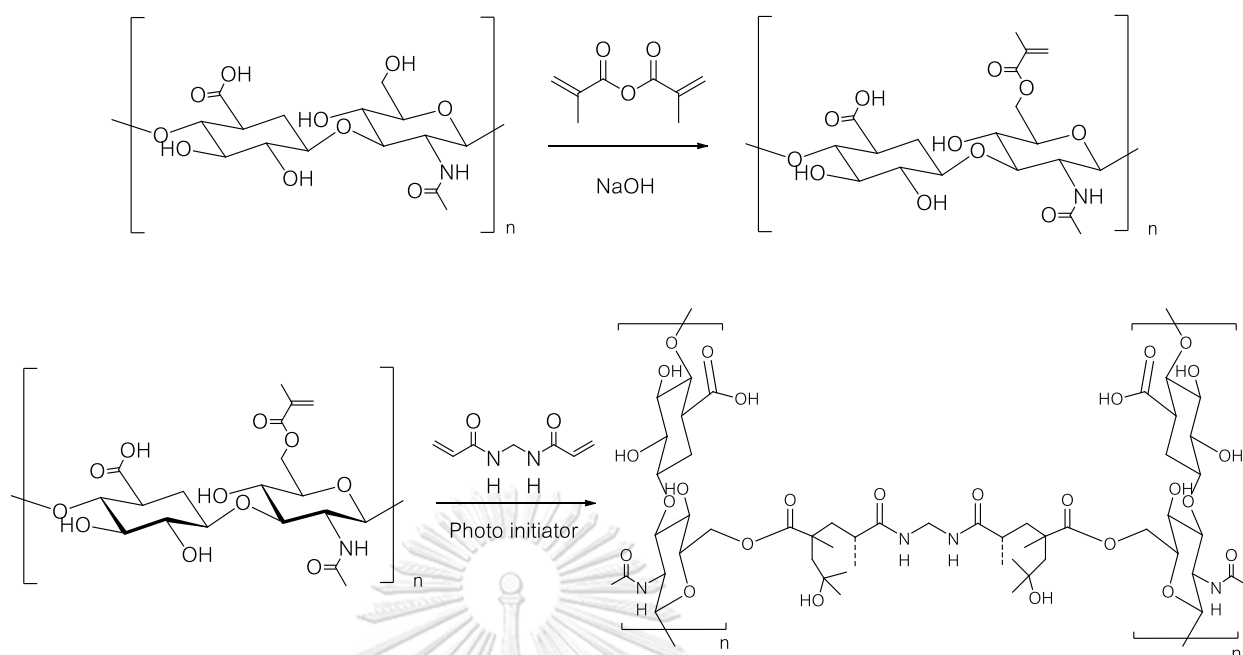


Figure 1. 2 Schematic of the HA crosslinking reaction *via* radical polymerization reaction

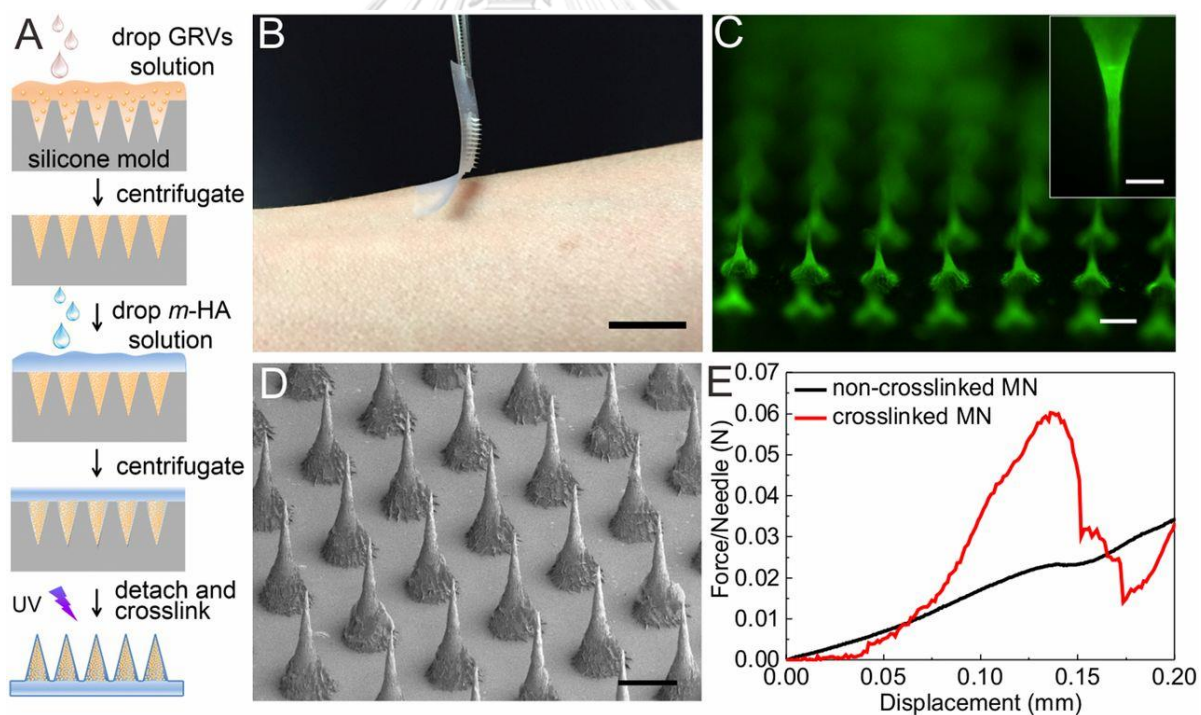


Figure 1. 3 Characterization of the HA microneedles patches. Schematic of the fabrication process of microneedles patch (A), photograph of the microneedles patch (B), fluorescence microscopy image of fluorescein-labeled insulin loaded microneedles patch (C), SEM image of microneedles patch (D), mechanical characteristic of non-crosslinked and crosslinked microneedles patches.⁵

1.2.2.2 PVP microneedles patches

PVP has been reported as a material for fabricating dissolvable microneedles patch. It has excellent biocompatibility and water solubility especially the PVP with a molecular weight less than 20 kDa. It is efficiently removed from kidneys after the injection. Therefore, it has been used for several purpose such as coating agent, polymeric membrane, and material for controlled drug release. PVP has a rapid dissolution rate in the skin.¹³

In 2017, Lee and co-worker fabricated dissolvable microneedles patches for insulin delivery with two molecular weights of PVP (360 kDa and 10 kDa). They found that PVP microneedles patch can puncture the porcine skin (Figure 1.4 A1-A4).

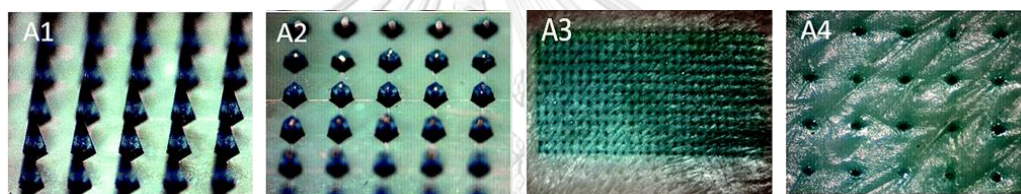


Figure 1. 4 *In vitro* skin insertion capability of Lissamine green B loaded PVP microneedles patch. Stereomicroscopy images of microneedles before insertion (A1), after insertion (A2). Porcine skin after the insertion of Lissamine green B loaded PVP microneedles patch (A3-A4)

1.2.2.3 PVP-PVA microneedles patches

The polymer with rapid dissolution rate may not be suitable for some applications that require long sustained release time such as hormone or vaccine deliveries.⁴ Thus, polymer blend may be used to create a new material that match the needs.

In 2015, Lee and co-worker fabricated PVP-PVA polymer blend microneedles patch at various polymer ratios to achieve microneedles with tunable dissolution rate. They found that the dissolution rate of microneedles could be controlled

by adjusting the ratio between PVP and PVA. The microneedles with higher PVP content show faster drug release than the microneedles with lower PVP content (Figure 1.5).

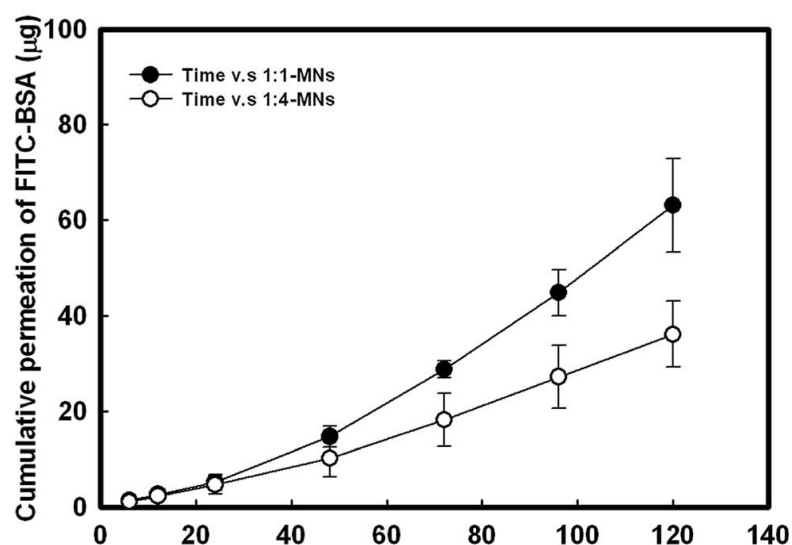


Figure 1. 5 *In vitro* drug-release profiles of fluorescein-labeled bovine serum albumin loaded PVP–PVA = 1:1 and PVP–PVA = 1:4 microneedles patch⁴

1.3 Objective

This research focused on developing HA/PVP polymer blend microneedle patches for transdermal drug delivery. Relationship between mechanical strength of the microneedles and ratios of HA and PVP were investigated. The study also includes the synthesis of acrylate modified HA and the used of acrylate modified HA to make crosslinked-HA-microneedles. The skin penetration ability and the dissolution rate of microneedles were studies in porcine ear skin. Loading of particulate drug in the obtained microneedle was also demonstrated.

CHAPTER II

EXPERIMENTAL

2.1 Materials and chemicals

The commercial polydimethylsiloxane (PDMS) microneedle molds were purchased from Micropoint Technologies Pte, Ltd. (Singapore), hyaluronic acid (cosmetic grade, MW 2 MDa) was purchased from Shandong Focuschem Biotech Co., Ltd. (Shandong Sheng, China), polyvinylpyrrolidone (analytical grade, MW 40 kDa), methacrylic anhydride (analytical grade) was purchased from Sigma-Aldrich (Missouri, USA), 2-hydroxy-4-(2-hydroxyethoxy)-2-methylpropiophenone (analytical grade) was purchased from Tokyo Chemical Industry Co., Ltd. (Tokyo, Japan), N,N'-Methylenebisacrylamide (analytical grade) was purchased from Merck KGaA (Darmstadt, Germany), black food coloring (food grade) was purchased from Greenhill Co., Ltd. (Bangkok, Thailand), retinal was purchase from Shanghai T&W Pharmaceutical Co., Ltd. (Shanghai, China), ethanol (commercial grade) was purchase from RCI Labscan Ltd. (Bangkok, Thailand). All chemicals were used without further purification.

2.2 Instruments and equipment

Morphology of microneedle patch was observed by stereomicroscope (Olympus DP22, Olympus Corporation, Tokyo, Japan) and scanning electron microscope (JEOL, Tokyo, Japan). Freeze-drying was carried out by Freeze-dry/Shell Freeze System Model 7753501 (Labconco Corporation, Kansas, MI, USA). Structure and degree of substitution of m-HA were evaluated by NMR spectrometer (Varian Mercury 400, Varian Company, USA). The mechanical properties were measured by universal testing machine (Shimadzu EZ-S, Shimadzu Corporation, Tokyo, Japan) and shore A durometer.

2.3 Fabrication of HA/PVP microneedle patches

HA/PVP microneedle patches were fabricated by micromolding process. First, five different composites of hyaluronic acid (HA)/ polyvinylpyrrolidone (PVP) polymer solution were prepared as shown in **Table 2.1**.

Table 2. 1 The amount of polymer for the preparation of HA/PVP solution

Sample Names	HA (mg)	PVP (mg)	DI Water (mL)
HA	1,000	0	10
HA/PVP at 75/25	750	250	10
HA/PVP at 50/50	500	500	10
HA/PVP at 25/75	250	750	10
PVP	0	1,000	10

After that, 0.1 mL of polymer solution (**Table 2.1**) was poured into the microneedle molds, then dried in desiccator overnight. Finally, adhesive tape was pasted on the microneedle as a supporting layer and the microneedle was pulled out from the mold. Morphology of HA/PVP microneedle patch was observed by stereomicroscope and scanning electron microscope.

2.5 Synthesis and characterization of acrylate modified HA

Acrylate modified HA (m-HA) was synthesized following the literature.¹ First, 2.0 g of HA was dissolved in 100 mL of deionized water and stirred at 4 °C. Then, 1.6 mL of methacrylic anhydride (MA) was added drop-wise. The reaction solution was adjusted to pH 8-9 by the addition of 5 M NaOH and stirred at 4 °C for 24 h. After that, the polymer was obtained by precipitation in acetone. The polymer was re-dissolved in deionized water and the polymer solution was dialyzed against deionized water for 2 days. Lastly, the product was obtained by Freeze-drying technique. The obtained product was characterized by ¹H NMR.

2.6 Fabrication of crosslinked-HA-microneedle patches

The crosslinked-HA-microneedle patches were prepared *via* radical polymerization by adjusting the ratios of m-HA, N,N'-Methylenebisacrylamide (MBA) and 2-hydroxy-4-(2-hydroxyethoxy)-2-methylpropiophenone (Photo initiator) and the irradiation time (UV light at 365 nm) as shown in **Table 2.2**.

Table 2. 2 The amount of reagents for the preparation of m-HA solution

Sample Name	m-HA (mg)	MBA (mg)	Photo initiator(mg)	Irradiation time(s)	DI Water (mL)
m-HA-1	80	80	1	5	2
m-HA-2	80	40	1	5	2
m-HA-3	80	80	1	10	2
m-HA-4	80	40	1	10	2
m-HA-5	80	40	2	5	2
m-HA-6	80	40	10	5	2
m-HA-7	80	40	20	5	2

First, 0.1 mL of m-HA solution (**Table 2.2**) was poured into the PVA coated microneedle molds. The polymer was crosslinked through radical polymerization by exposure to UV light at the specific time (**Table 2.2**). Then, The polymer was dried in desiccator overnight. Morphology of HA/PVP microneedle patches were observed by stereomicroscope.

2.7 Mechanical testing of HA/PVP microneedle patches

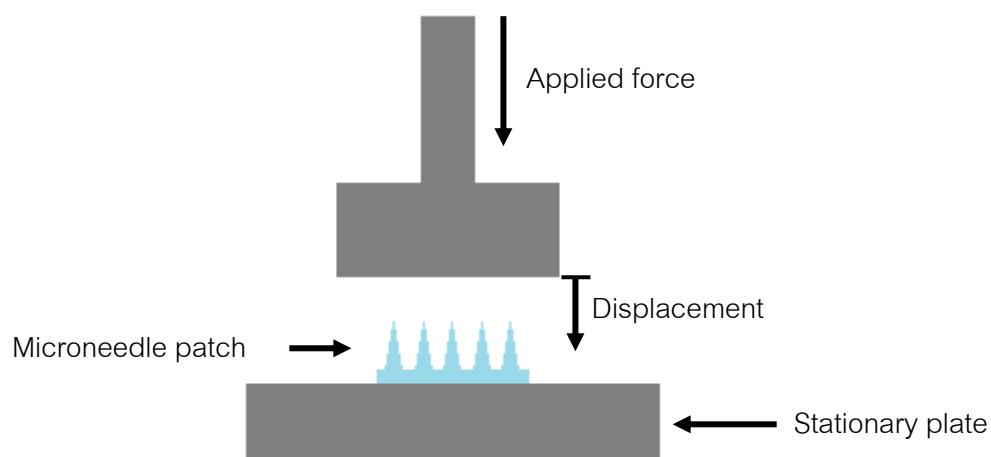


Figure 2. 1 Schematic setup of compression test of HA/PVP microneedle performed by UTM

The compressive strength of HA/PVP microneedle patches was measured by universal testing machine. First, the needles were placed on the stationary plate with the needles facing up (Figure 2.1). Another stainless-steel plate was moved toward the needles at a rate of 1 mm/min until a maximum load of 100 N was obtained or until the failure force of microneedle was recorded. Morphology of HA/PVP microneedle patches were observed before and after compressive testing by stereomicroscope and SEM.

The polymer was casted into a film and measure the hardness compare to the human skin by shore A durometer.

2.8 *Ex vivo* skin penetration test of HA/PVP microneedle patches

Black food coloring was mixed into the polymer solution (Table 2.1) to give colored needles under microscope. The colored HA/PVP microneedle patch was applied to porcine ear skin. The images of needles penetration were observed by stereomicroscope.

2.9 *In situ* dissolution rate of microneedle in porcine ear skin

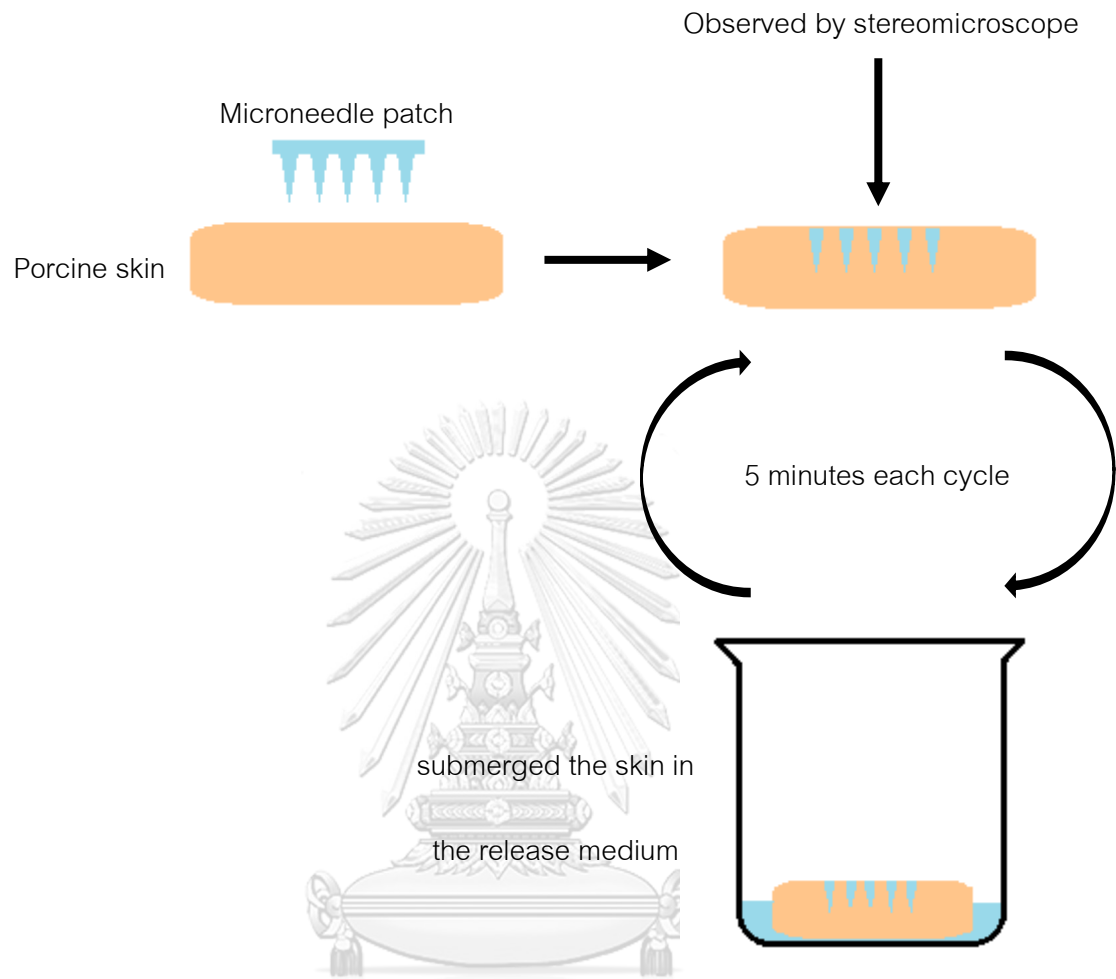


Figure 2. 2 Schematic of *in situ* dissolution rate of microneedle in porcine ear skin testing

Black food coloring was mixed into the polymer solution (Table 2.1) to give colored needles under microscope. Only the microneedle with the ability to penetrate the skin were studied (HA/PVP at 50/50, HA/PVP at 25/75 and PVP microneedle). The microneedle patch was applied to the porcine skin. Then, the images of the needles in the skin were observed after submerging the skin in the release medium every 5 minutes until the color completely disappeared (Figure 2.2).

2.10 Fabrication of retinal loaded HA/PVP microneedle patches

HA/PVP at 50/50 was chosen as a representative for fabricate retinal loaded HA/PVP microneedle patches. First, 500 mg of HA and 500 mg of PVP were dissolved in

10 mL of deionized water. Then, of 60 mg of retinal in 5 mL of ethanol was added to the polymer solution and the solution was stirred at room temperature until the solution was homogeneous. Then, 0.1 mL of polymer solution was poured into the PVA coated microneedle molds and dried in desiccator overnight. Finally, adhesive tape was pasted on the microneedle as a supporting layer and the microneedle was pulled out from the mold. Morphology of retinal loaded HA/PVP microneedle patch was observed by stereomicroscope and scanning electron microscope. The mechanical properties of retinal loaded HA/PVP microneedle patch were measured compare to HA/PVP microneedle patch by universal testing machine and shore A durometer.



CHAPTER III

RESULTS AND DISCUSSIONS

3.1 Fabrication of HA/PVP microneedle patches

The HA/PVP microneedle patches were fabricated by micromolding process.

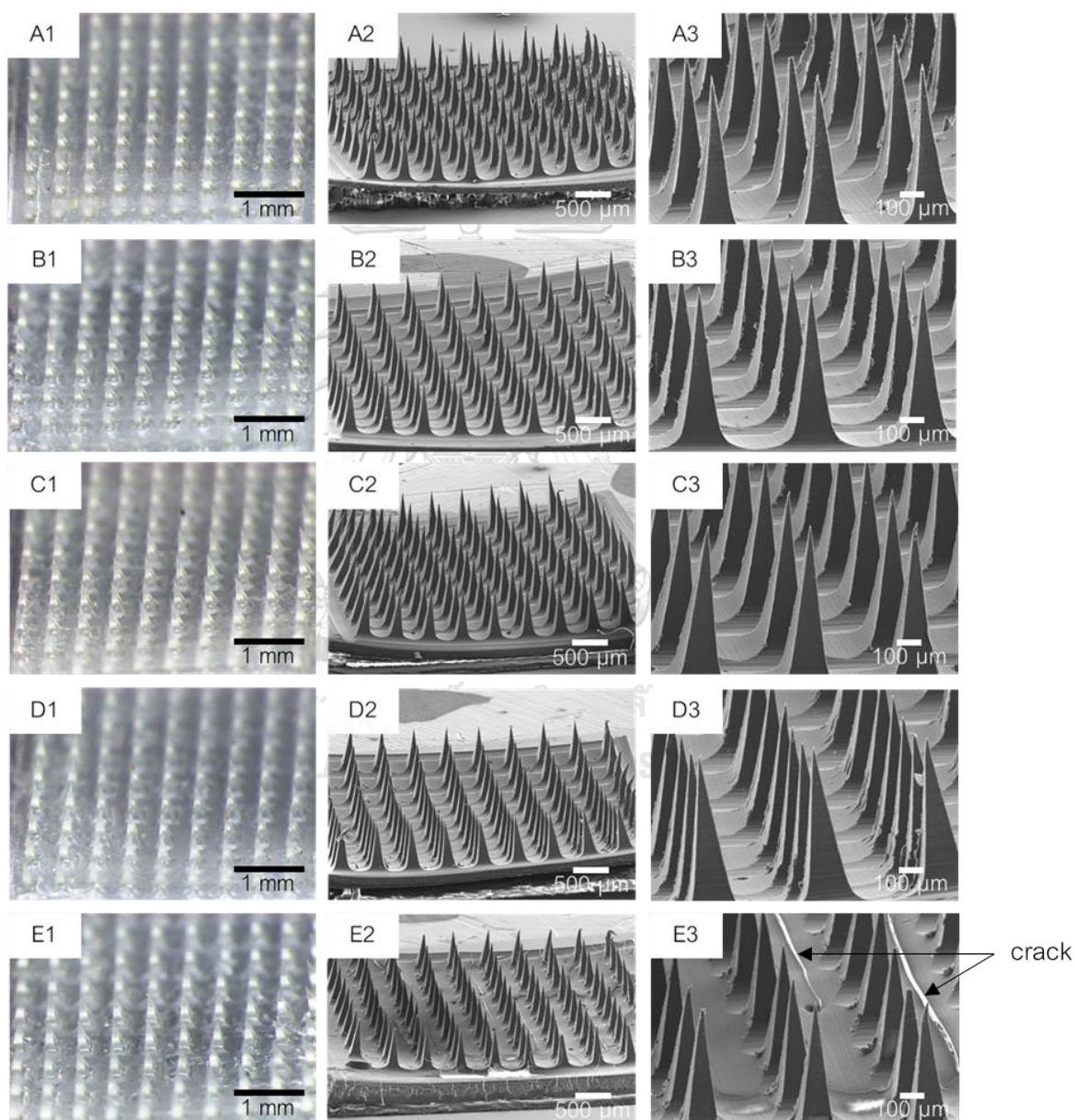


Figure 3. 1 Stereomicroscopic and SEM images of HA/PVP microneedle patches made of (A) HA, (B) HA/PVP at 75/25, (C) HA/PVP at 50/50, (D) HA/PVP at 25/75, (E) PVP.

The PDMS mold with pyramidal microneedle was chosen because previous literature has revealed that pyramidal microneedle shows better mechanical strength than conical type microneedle. This shape helps for the microneedle fabricated from the relatively mechanically weak biomaterials to have good skin penetration.⁸ Five different composites of HA/PVP microneedle patches (HA/PVP at 100/0, 75/25, 50/50, 25/50, 0/100) were fabricated as described in section 2.4. **Figure 3.1 (A)-(E)** show the five composite microneedles. **Figure 3.1 (E1)-(E3)** reveal that only patches with 100% PVP possess some fractures on the base. It was concluded that PVP alone is not suitable for the fabrication of microneedle patch and the HA is needed.

3.2 Synthesis and characterization of acrylate modified HA (m-HA)

Acrylate was introduced to the HA chain as a crosslinking functional group. The acrylate-containing HA (m-HA) was synthesized by esterification reaction.

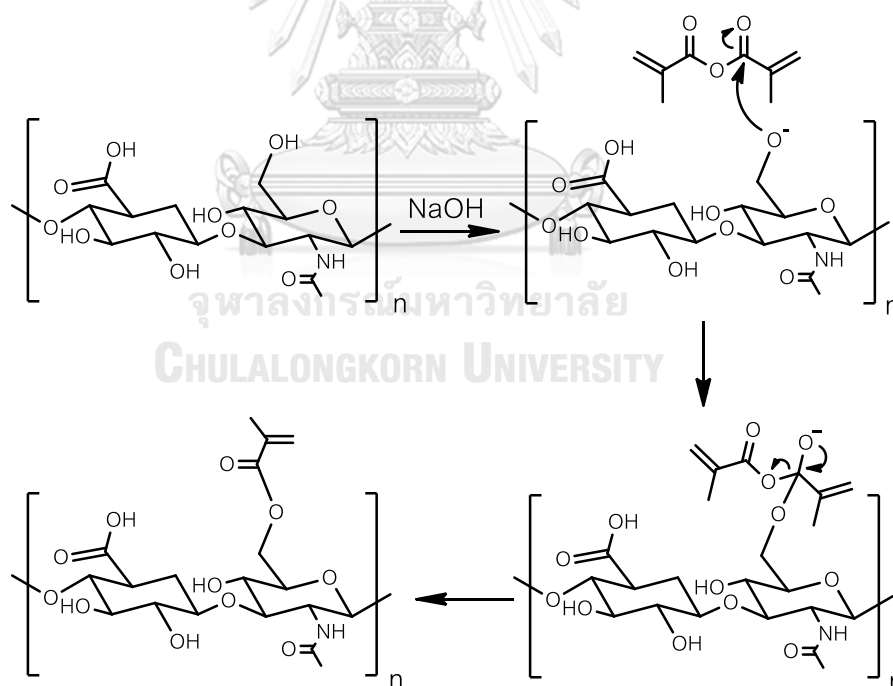


Figure 3. 2 The mechanism of m-HA *via* esterification reaction.

The mechanism is proposed as follow: 1) hydroxyl group (-OH) of HA was deprotonated by NaOH generating ethoxy functional group, 2) the alkoxy functional

group acts as a nucleophile and attack the carbonyl carbon of methacrylic anhydride, 3) forming negative charged tetrahedral intermediate that splits into product by eliminating 2-methylacrylate. Electron push diagram is shown in **Figure 3.2**.

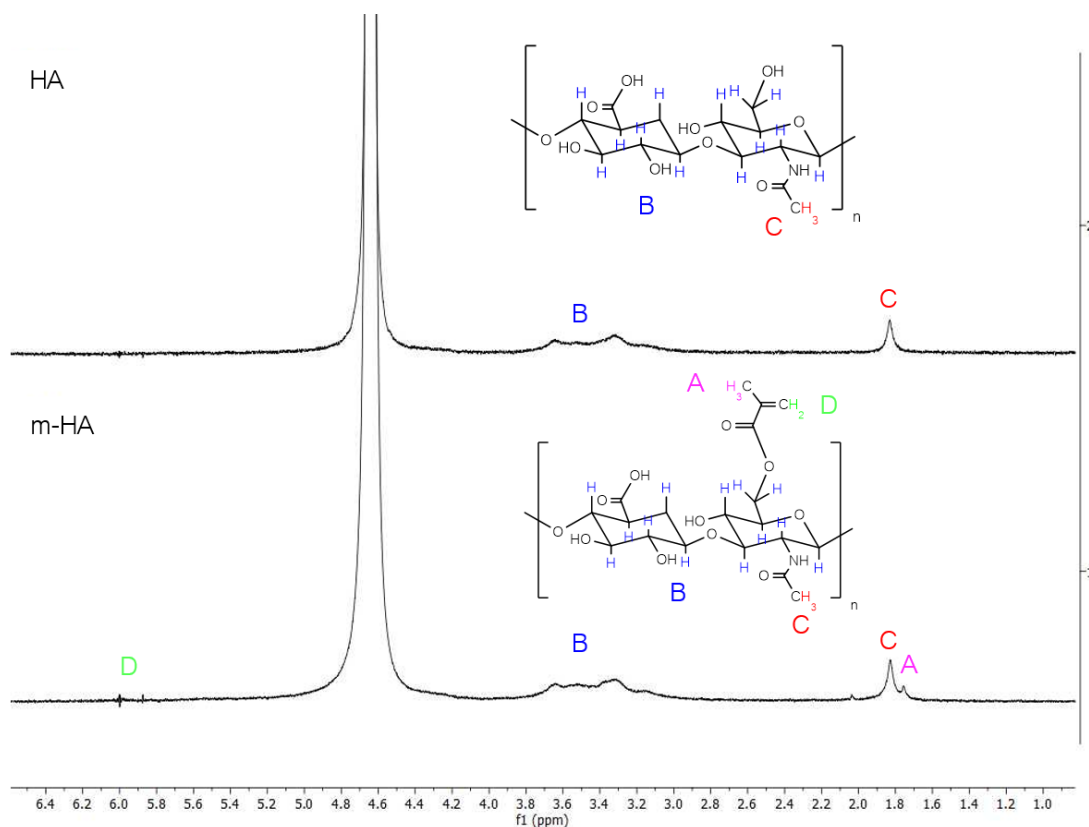


Figure 3.3 ^1H NMR spectra of HA, and m-HA in D_2O .

NMR spectrum of HA (**Figure 3.3** HA) shows signal at 1.83 ppm (s, 3H) which indicates the protons of *N*-acetyl glucosamine of HA (NHCOCH_3). The signals between 3.00 to 3.80 ppm correspond to the proton in the sugar ring of HA monomer units. The NMR spectrum of m-HA (**Figure 3.3** m-HA) shows signal at 1.83 ppm (s, 3H) which indicates the proton of *N*-acetyl glucosamine of HA (NHCOCH_3). The signals between 3.00 ppm to 3.80 ppm correspond to the proton in the sugar ring of HA monomer units. The signals at 1.75 ppm (s, 3H) correspond to proton of methyl group of methacrylate ($\text{CH}_2=\text{C}(\text{CH}_3)\text{CO}$). The signal at 5.87 ppm (s, 1H) and 6.00 ppm (s, 1H) correspond to methacrylate proton ($\text{CH}_1\text{H}_2=\text{C}(\text{CH}_3)\text{CO}$). The degree of substitution calculated from

ratio of the areas under the proton peaks at 1.77 ppm (methyl proton of methacrylate) to the peak at 1.82 ppm (methyl proton of N-acetyl glucosamine of HA) was 28%.

3.3 Fabrication of crosslinked-HA-microneedle patches

The crosslinked-HA-microneedle patches were prepared *via* radical polymerization. In this work, we varied the amount of m-HA, N,N'-Methylenebisacrylamide (MBA) and 2-hydroxy-4-(2-hydroxyethoxy)-2-methylpropiophenone (Photo initiator) and the irradiation time (UV light at 365 nm). The mechanism (Figure 3.4) is proposed as follow: 1) the photo initiator is exposure to UV light at 365 nm, the bond between the quaternary carbon and the carbonyl carbon is cleaved heterolytically, and the radical initiator is formed, 2) the radical initiator attacks the π bond on the m-HA chain, forming a bond with carbon atom and starting the chain reaction by turning the m-HA into another radical, 3) the propagation step where the radical on m-HA chain attacks pi bond on MBA and forms a bond with MBA, 4) the radical on another m-HA molecule attacks π bond on the other side of the MBA and forms a crosslinked m-HA, 5) the chain termination can occur by several mechanisms. The radical can react with initiator radical or another radical chain to terminate the reaction.

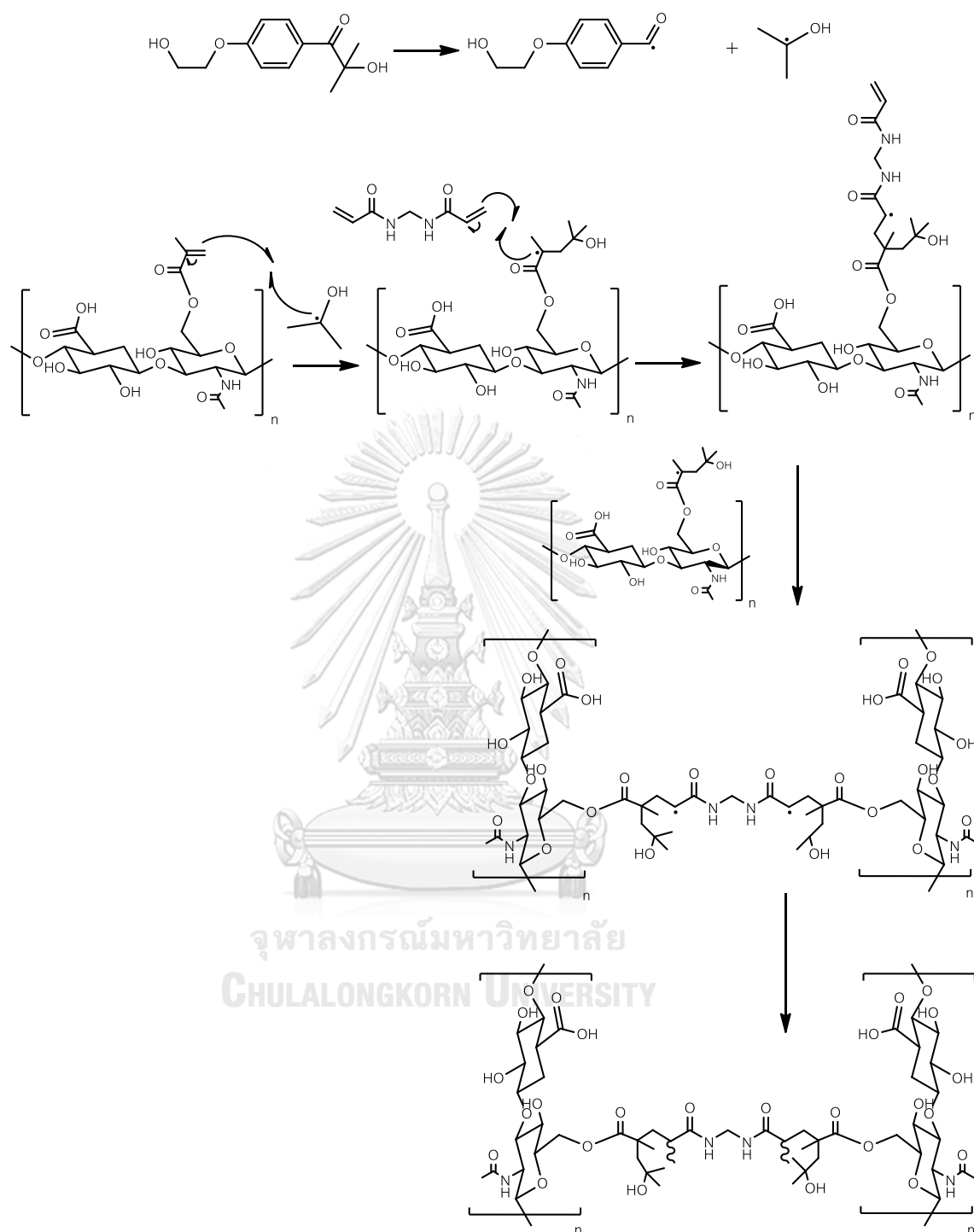


Figure 3. 4 The mechanism of crosslinked m-HA via esterification reaction.

Table 3. 1 Appearance of the products formed under different Crosslinking conditions

Name	m-HA (mg)	MBA (mg)	Photo initiator (mg)	Irradiation time (s)	Appearance
m-HA-1	80	80	1	5	White powder
m-HA-2	80	40	1	5	White powder
m-HA-3	80	80	1	10	White powder
m-HA-4	80	40	1	10	White powder
m-HA-5	80	40	2	5	White powder
m-HA-6	80	40	10	5	Solid material with shrinking volume and white powder
m-HA-7	80	40	20	5	Solid material with shrinking volume

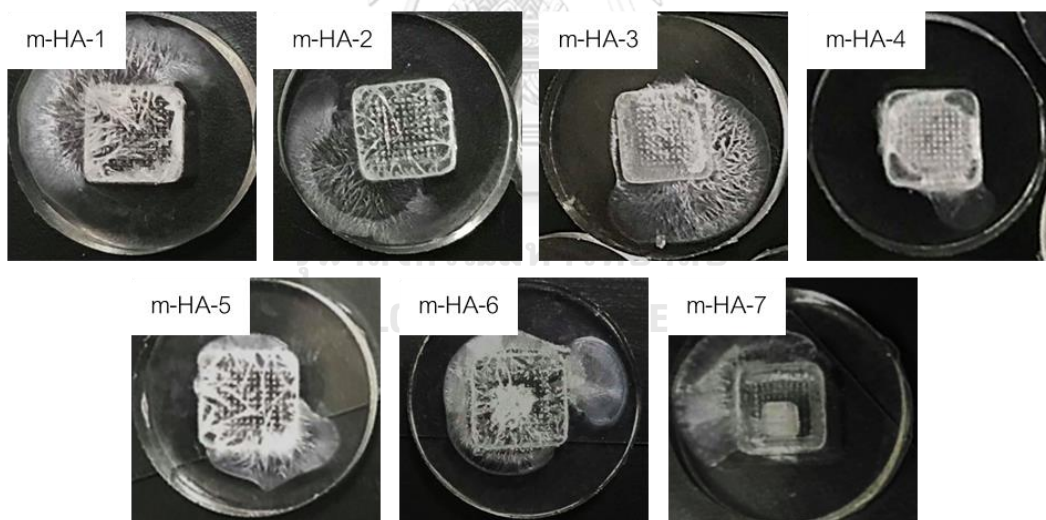


Figure 3. 5 The image of m-HA microneedle patches fabricated under difference conditions as shown in table 1.1.

First, we started with the same condition as literature (Table 3.1 m-HA-1).⁵ We found that in this condition, there was white powder of MBA after the polymer dried. Then, we tried the condition with half of the MBA (m-HA-2). We found that there was also white powder, but the amount was reduced. It was likely that the crosslinking reaction

did not take place with all the m-HA. After that, we increased the irradiation time from 5 to 10 minutes (Figure 3.5 and Table 3.1 m-HA-3, and m-HA-4). The product still appeared as a white powder. Then, we tried to increase the amount of photo initiator from 1 to 2, 10 and 20 (Figure 3.5 and Table 3.1 m-HA-5, H-HA-6, and m-HA-7). There were crosslinked-HA appear in m-HA-6 in the center of patch but there was still some MBA remained. For m-HA-7, the solid product was obtained but its volume was shrunken (less than the volume of the mold).

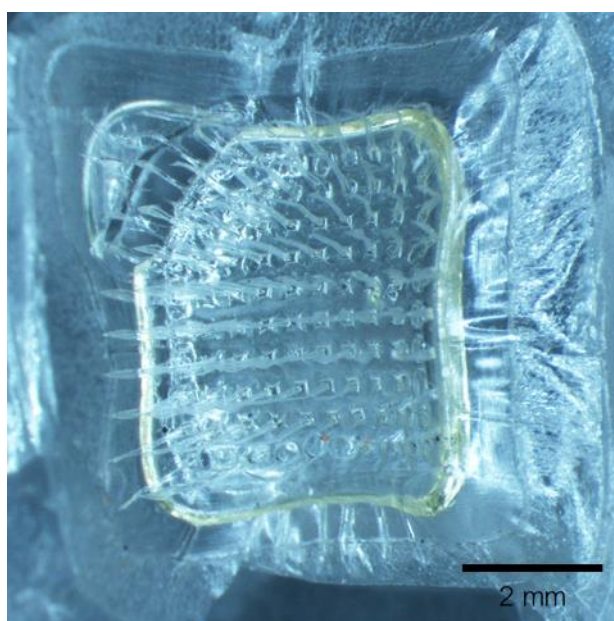


Figure 3. 6 Stereomicroscopic image of crosslinked-HA-microneedle patches.

The stereoscopic image of m-HA-7 (Figure3.6) reveals solid product with reduced dimension comparing to the dimension of the mold. We speculate that the crosslinking reaction produced very compact molecular arrangement, then the volume of the solid product was lesser than the usual product obtained with non-crosslinked fabrication process described earlier. Since we have already tried out the fabrication at lower concentration of the crosslinking agent and could not obtain solidify product, the other option left for the tryout of the crosslinking process is the variation of HA molecular weight. Nevertheless, due to the high price of low molecular weight HA, we decided to use the non-crosslink method and abandon the crosslinking process.

3.4 Mechanical testing of HA/PVP microneedle patches

Measurement of mechanical strength of each microneedle patch was carried out using a universal testing machine. A plot of force versus displacement was then constructed. The morphology of HA/PVP microneedle patches after being compressed was observed by stereomicroscope and SEM.

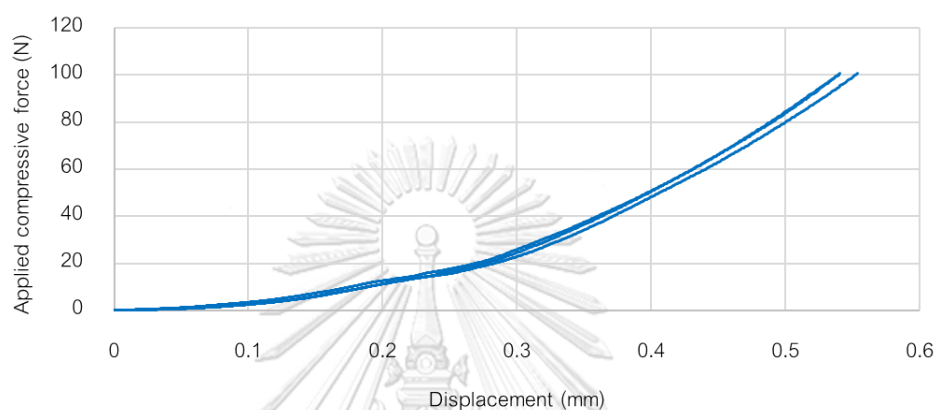


Figure 3. 7 Mechanical characteristic of HA microneedle patch.

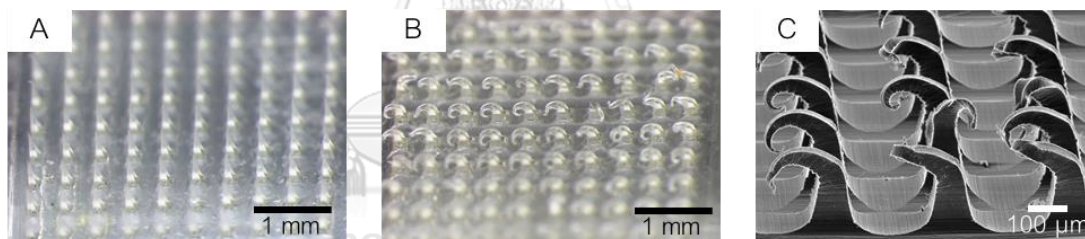


Figure 3. 8 Stereomicroscopic images of HA microneedle patch (A) before and (B) after the compressive test. SEM image of the HA microneedle patch after the compressive test is shown in (C).

The mechanical characteristic of HA microneedle patch (Figure 3.7) exhibits a second-degree harmonic relationship between the applied compressive force and the displaced distance. The smooth graph indicates that no fracture was taking place during the compression test. The images of HA microneedle patch (Figure 3.8) indicate the bend at the needle tip. Such bending likely contributed to the harmonic increase in the compressive force along the displaced distance (distance progressed from the needle bend).

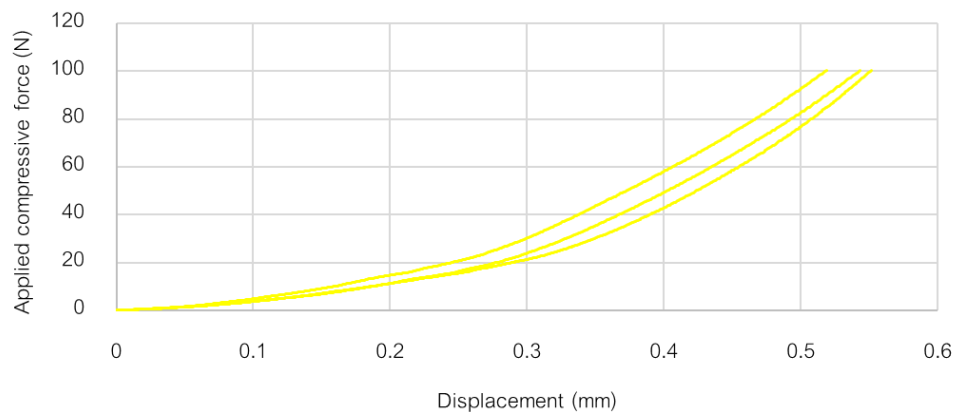


Figure 3. 9 Mechanical characteristic of HA/PVP at 75/25 microneedle patch.

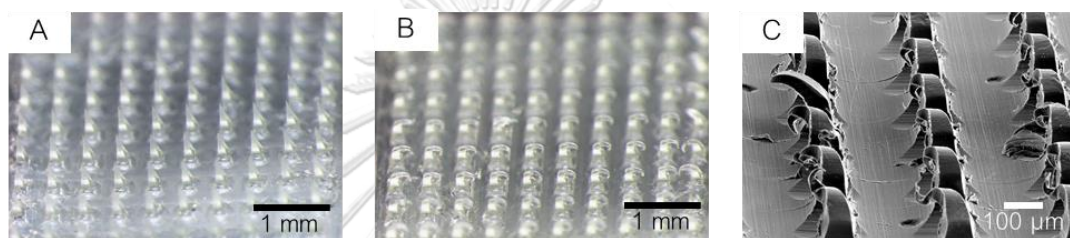


Figure 3. 10 Stereomicroscopic images of 75/25 HA/PVP microneedle patch (A) before and (B) after the compressive test. SEM image of the 75/25 HA/PVP microneedle patch after the compressive test (C).

The mechanical characteristic of 75/25 HA/PVP microneedle patch (Figure 3.9) exhibits a second-degree harmonic relationship between the applied compressive force and the displaced distance. The smooth graph indicates that no fracture was taking place during the compression test. The images of 75/25 HA/PVP microneedle patch (Figure 3.10) indicate bending of the needle during the compression. Such bending likely contributed to the harmonic increase in the compressive force along the displaced distance (distance progressed from the needle bend).

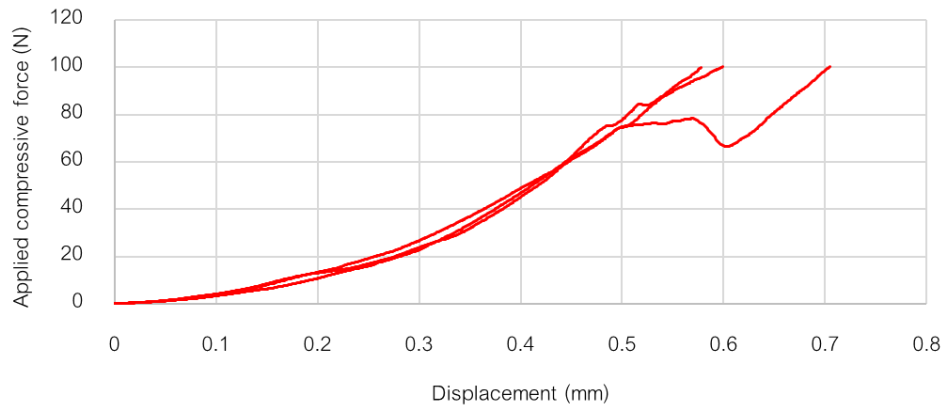


Figure 3. 11 Mechanical characteristic of HA/PVP at 50/50 microneedle patch.

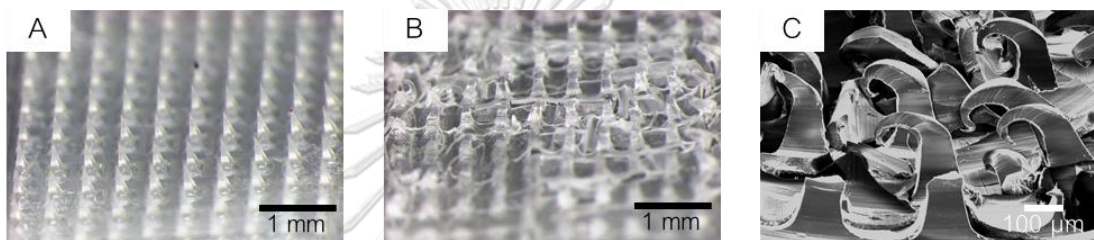


Figure 3. 12 Stereomicroscopic images of 50/50 HA/PVP microneedle patch (A) before and (B) after the compressive test. SEM image of the 50/50 HA/PVP microneedle patch after the compressive test (C).

Mechanical characteristic of 50/50 HA/PVP microneedle patch (Figure 3.11) is shown as a graph between applied compressive force and displaced distance. Harmonic at the order of two was observed between applied compressive force and displaced distance up to the force of 80 N. At the force over 80 N, the abrupt drop in the force needed with progressing distance was observed. This indicate the crack of the tested sample. The image of 50/50 HA/PVP microneedle patch (Figure 3.12) shows both the crack and the bend of the needles.

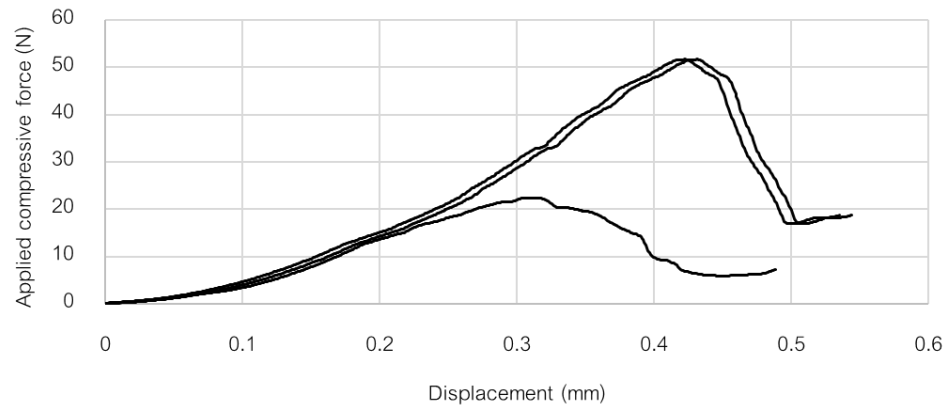


Figure 3. 13 Mechanical characteristic of HA/PVP at 25/75 microneedle patch.

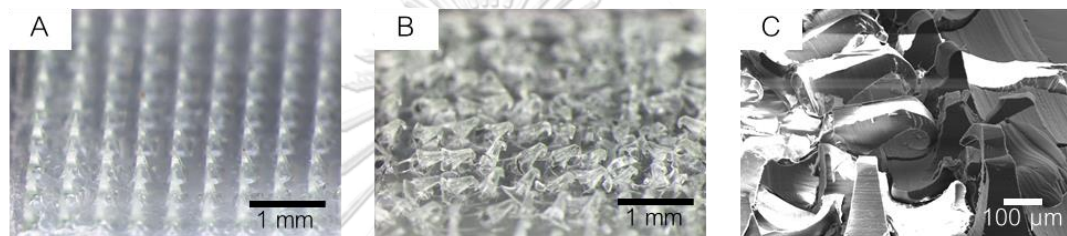


Figure 3. 14 Stereomicroscopic images of 25/75 HA/PVP microneedle patch (A) before and (B) after the compressive test. SEM image of the 25/75 HA/PVP microneedle patch after the compressive test (C).

The mechanical characteristic of 25/75 HA/PVP microneedle patch (Figure 3.13) is shown as a graph between applied compressive force and displaced distance. Harmonic at the order of two was observed between applied compressive force and displaced distance up to the force of 50 N. At the force over 50 N, the abrupt drop in the force needed with progressing distance was observed. This indicates the crack of the tested sample. The image of 25/75 HA/PVP microneedle patch (Figure 3.14) shows both the crack and the bend of the needles.

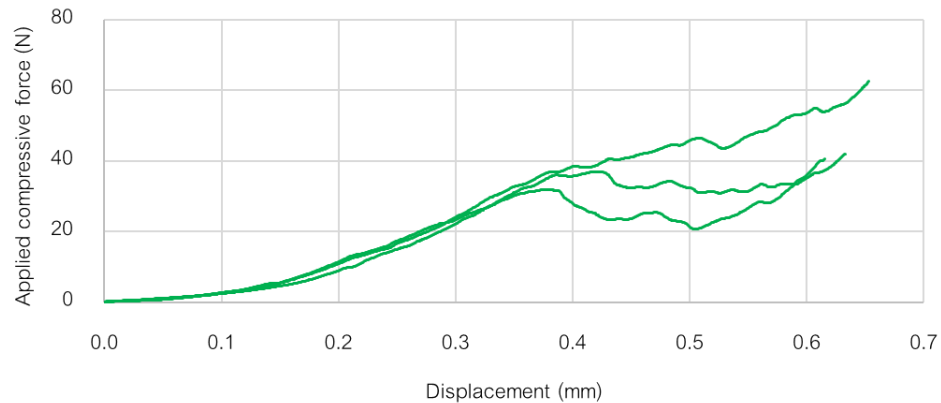


Figure 3. 15 Mechanical characteristic of PVP microneedle patch.

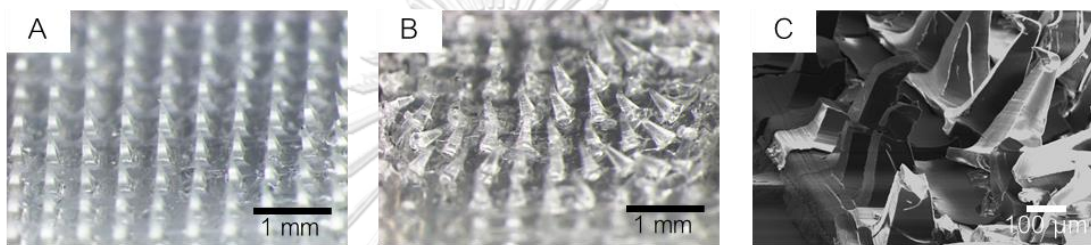


Figure 3. 16 Stereomicroscopic images of PVP microneedle patch (A) before and (B) after the compressive test. SEM image of the PVP microneedle patch after the compressive test (C).

The mechanical characteristic of PVP microneedle patch (Figure 3.15) is shown as a graph between applied compressive force and displaced distance. Harmonic at the order of two was observed between applied compressive force and displaced distance up to the force of 40 N. At the force over 40 N, the abrupt drop in the force needed with progressing distance was observed. This indicates the crack of the tested sample. The image of PVP microneedle patch (Figure 3.16) shows both the crack and the bend of the needles.

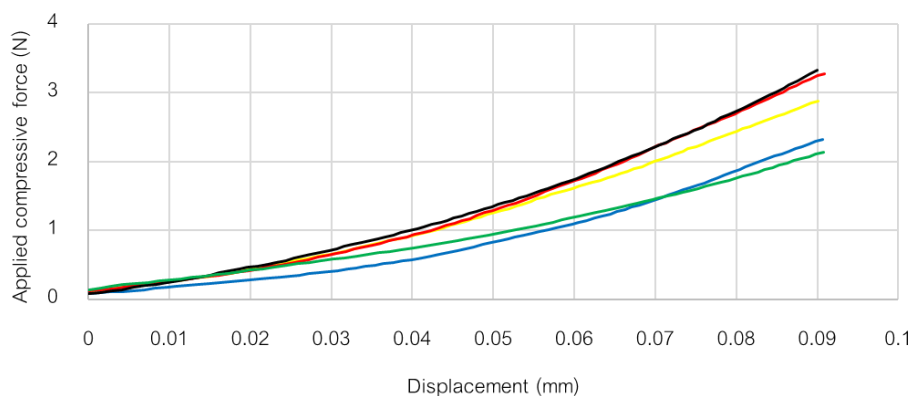


Figure 3. 17 Mechanical characteristic of different microneedle patches: HA (blue), 75/25 HA/PVP (yellow), 50/50 HA/PVP (red), 25/75 HA/PVP (black), and PVP (green).

Table 3. 2 Shore A hardness of different polymer films and skin

Film formula	Shore A hardness
HA	91.1 ± 1.3
HA/PVP at 75/25	89.8 ± 3.5
HA/PVP at 50/50	90.0 ± 1.8
HA/PVP at 25/75	89.6 ± 1.4
PVP	89.7 ± 1.4
Skin	9.1 ± 1.5

As shown in **Figure 3.17**, microneedle patches with higher PVP content (25/75 and 50/50 HA/PVP) possessed a higher compressive strength. This result conforms to the rigid ring structure of vinyl pyrrolidone.¹³ However, PVP alone showed similar character up to the force around 0.5 N. The needle shows less resistance to the higher force when compare to needles with HA composition. We speculate that microcracking might take place. SEM image of the PVP patch post the compressive test agree well with the speculation. The shore A hardness of different polymer film shown in **Table 3.2** reveal no significant difference among patch with different PVP content. All the needle patches possess higher hardness than skin. This implies that microneedle patches made from these polymer compositions can piece the skin. Consequently, microneedle

patches made of HA, 75/25 HA/PVP, 50/50 HA/PVP, 25/75 HA/PVP, and PVP were further investigated for the skin penetration test using *ex vivo* porcine skin.

3.5 *Ex vivo* skin penetration test of HA/PVP microneedle patches

The black colored HA/PVP microneedle patches were fabricated for skin penetration test. The images of needles penetration were observed by stereomicroscope.

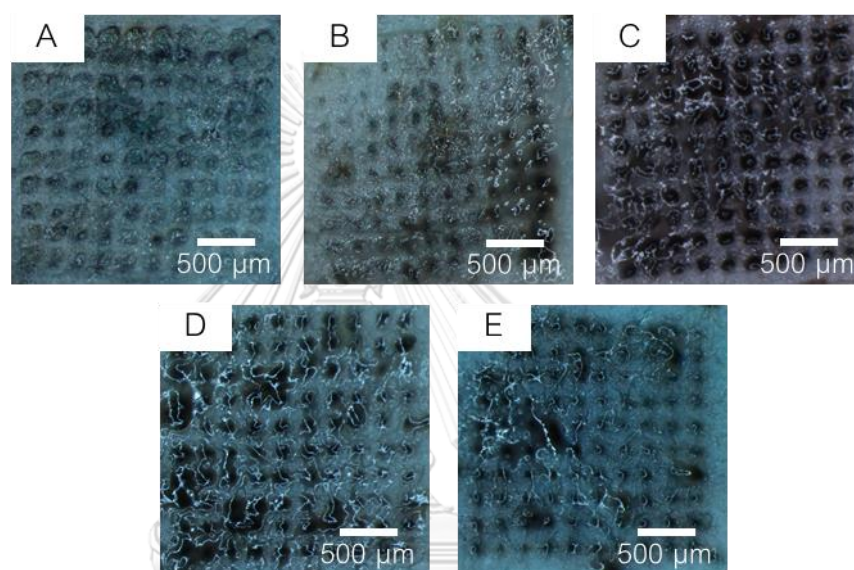


Figure 3.18 Top view of the *ex vivo* skin that had been treated with microneedle patches made of (A) HA, (B) 75/25 HA/PVP, (C) 50/50 HA/PVP, (D) 25/75 HA/PVP, and (E) PVP.

The top view of porcine skin post microneedle patch application (**Figure 3.18**) revealed the black color in the needle array pattern on the skin, indicating that the needles were successfully embedded in the skin. **Figure 3.18** (A) shows only 1-2 spots of the black color on the skin, indicating that HA microneedle cannot penetrate the skin effectively. This suggests that the un-crosslinked-HA has insufficient strength to puncture the skin. As shown in **Figure 3.18** (B), some black dots representing the penetration of some needles could be observed with the 75/25 HA/PVP microneedle patch. **Figure 3.18** (C) shows complete black dot array on the skin, indicating complete

embedding of all needles into the skin for the 50/50 HA/PVP microneedle patch. **Figure 3.18 (D)-(E)** show complete black dot array on the skin, indicating complete embedding of all needles into the skin for the 25/75 HA/PVP and PVP microneedle patch. However, the color of the needles left on the skin in **Figure 3.18 (D)-(E)** was less intense than that in **Figure 3.18 (C)**. It was possible that the needles with higher PVP content had higher dissolution rate. Therefore, the color faded faster. We conclude that needles made of 50/50 HA/PVP, 25/75 HA/PVP, and PVP could be embedded into the porcine skin, therefore these patches were further investigated for the dissolution rate in the porcine skin.

3.6 *In situ* dissolution rate of microneedle in porcine ear skin

The black colored HA/PVP microneedle patches were fabricated for this test. The patch was put onto the porcine skin. The images of the needles in the skin were taken every 5 min after submerging the skin in the release medium until the color completely disappeared (see method 2.9).

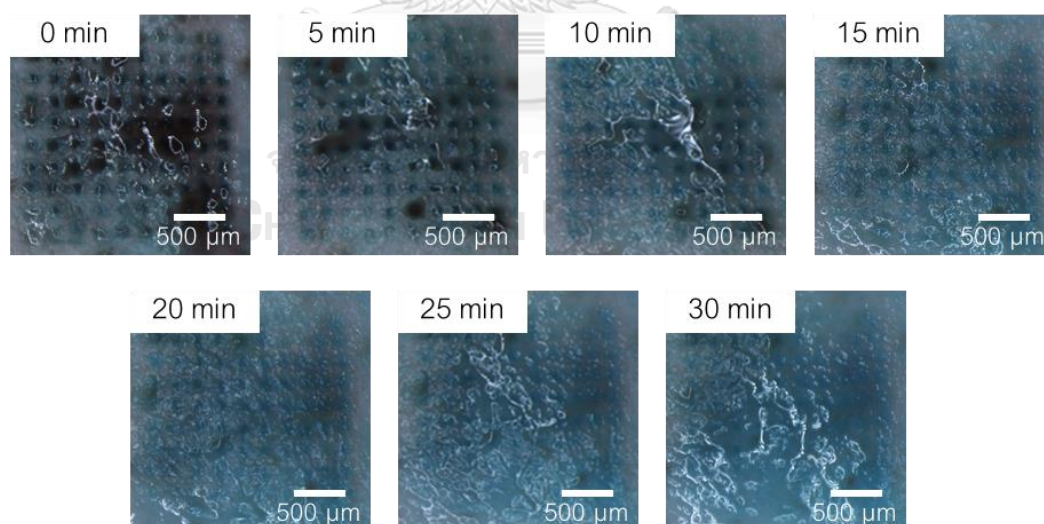


Figure 3. 19 The top view picture of porcine ear skin that had been treated with 50/50 HA/PVP microneedle patch and was submerged in release medium. Each picture shows the top view of the skin at various times post application.

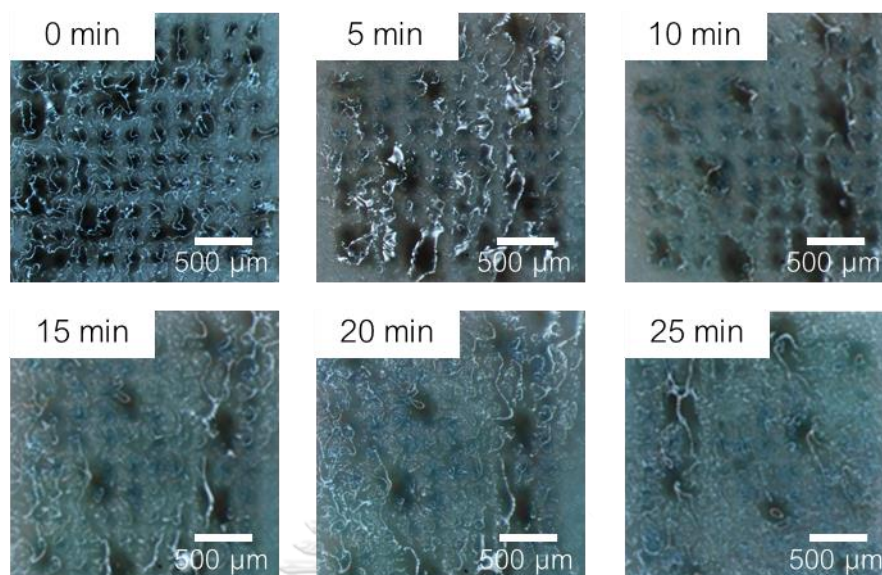


Figure 3. 20 The top view picture of porcine ear skin that had been treated with 25/75 HA/PVP microneedle patch and was submerged in release medium. Each picture shows the top view of the skin at various times post application.

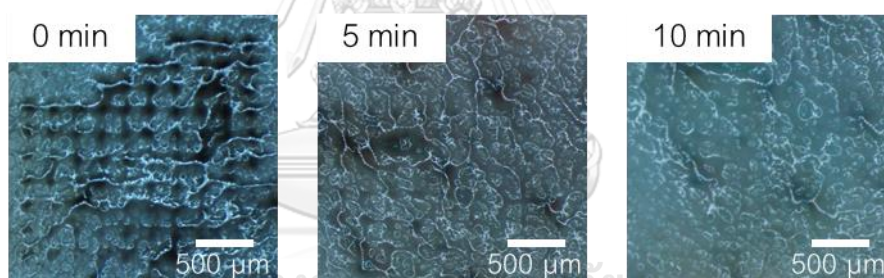


Figure 3. 21 The top view picture of porcine ear skin that had been treated with PVP microneedle patch and was submerged in release medium. Each picture shows the top view of the skin at various times post application.

The top view of porcine skin post microneedle patch application and submerged in release medium (Figure 3.19-3.21) revealed the different black spot fading rate in each composition, indicating that we could control the dissolution rate by varying the HA/PVP composition. Figure 3.19 shows black dot array was completely disappear after submerged in release medium for 30 min, indicating complete dissolving in skin of all needles in 30 min for 50/50 HA/PVP microneedle patch. As shown in Figure 3.20, shows black dot array was completely disappear after submerged in release medium for 25

min, indicating complete dissolving in skin of all needles in 25 min for 25/75 HA/PVP microneedle patch. **Figure 3.21**, shows black dot array was completely disappear after submerged in release medium for 10 min, indicating complete dissolving in skin of all needles in 10 min for PVP microneedle patch.

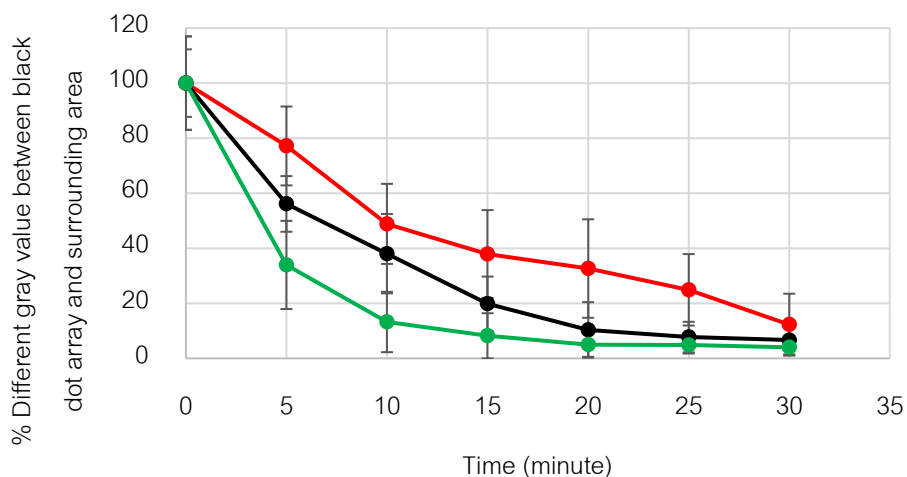


Figure 3. 22 Relationship between % different gray value between black dot array and surrounding area and time of 50/50 HA/PVP (red), 25/75 HA/PVP (black), and PVP (green) microneedle patches.

The relationship between % different gray value between black dot array and surrounding area and time (**Figure 3.22**) show microneedle patches with higher PVP content dissolve faster than microneedles patches with lower PVP content. It is considered that the lower molecular weight of PVP comparing to HA result in faster dissolution rate. We conclude that microneedle patches with higher PVP content possessed a higher dissolution rate.

3.7 Fabrication of retinal-loaded HA/PVP microneedle patches

The 50/50 HA/PVP was a chosen formulation used to fabricate retinal-loaded HA/PVP microneedle patches. **Figure 3.22** shows the picture of the fabricated microneedle patch. The picture indicates that we successfully fabricated the retinal-loaded HA/PVP microneedle patch.

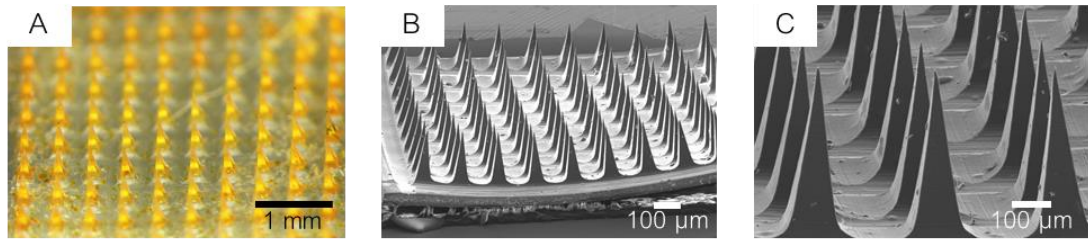


Figure 3. 23 Stereomicroscopic image of retinal-loaded HA/PVP microneedle patches (A) SEM image of retinal loaded HA/PVP microneedle patch (B-C).

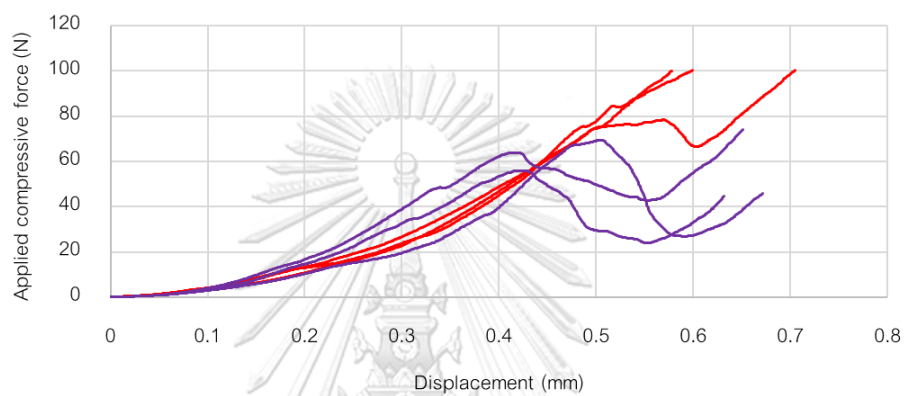


Figure 3. 24 Mechanical characteristic of 50/50 HA/PVP microneedle patches (red), retinal-loaded HA/PVP microneedle patches (purple).

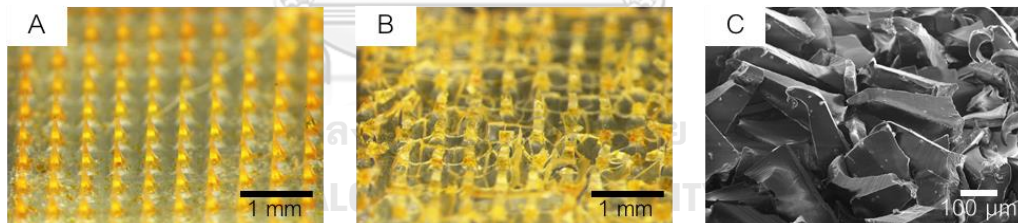


Figure 3. 25 Stereomicroscopic images of retinal loaded microneedle patch (A) after compressive test (B).

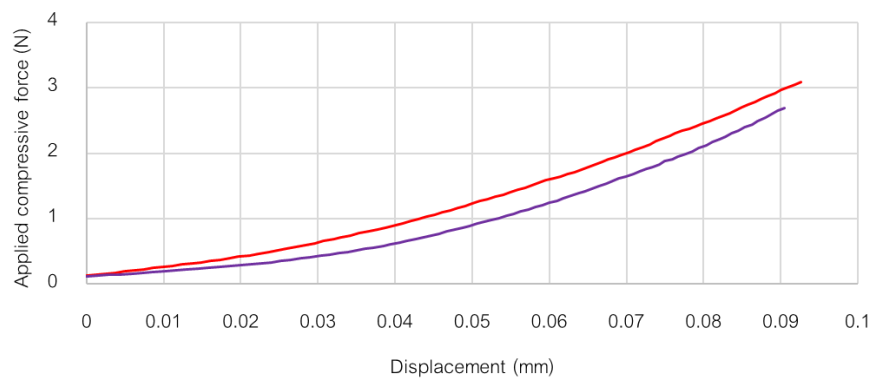
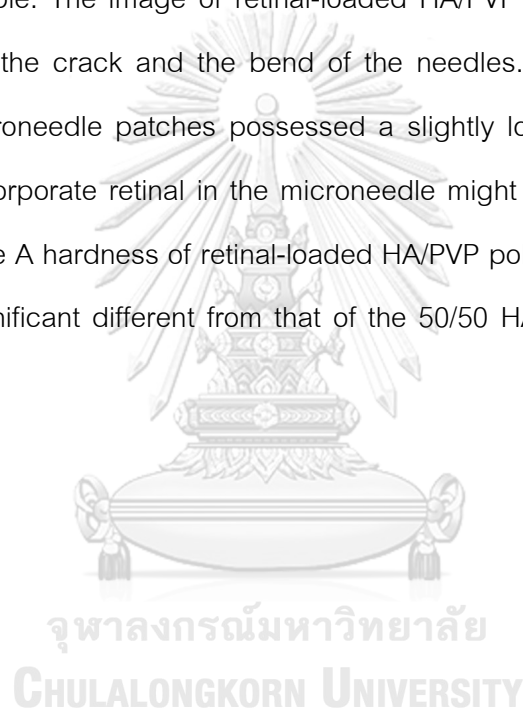


Figure 3. 26 Mechanical characteristic at the low displacement of 50/50 HA/PVP microneedle patches (red), retinal-loaded HA/PVP microneedle patches (purple).

Mechanical characteristic of retinal-loaded HA/PVP microneedle (**Figure 3.23** purple) is shown as a graph between applied compressive force and displaced distance. Harmonic at the order of two was observed between applied compressive force and displaced distance up to the force of 70 N. At the force > 70 N, the abrupt drop in the force needed with progressing distance was observe. This indicate the crack of the tested sample. The image of retinal-loaded HA/PVP microneedle patch (**Figure 3.24**) shows both the crack and the bend of the needles. As shown in **Figure 3.25**, retinal-loaded microneedle patches possessed a slightly lower compressive strength, indicating that incorporate retinal in the microneedle might decrease the compressive strength. The shore A hardness of retinal-loaded HA/PVP polymer film is 88.9 ± 4.0 . The number is not significant different from that of the 50/50 HA/PVP polymer film (90.0 ± 1.8).



CHAPER IV

CONCLUSION

We successfully prepared five composites of HA/PVP microneedle patches, the patches with HA/PVP at 100/0, 75/25, 50/50, 25/50, and 0/100. The mechanical properties measured by universal testing machine and durometer show that microneedle patches with higher PVP content possess a higher compressive strength. Although we have also successfully synthesized the acrylate modified HA to be used in the fabrication of crosslinked-HA microneedle, the crosslinked-HA microneedles could not be prepared due to shrinking problem. Only the microneedle patches made of non-crosslinked 50/50 HA/PVP, 25/75 HA/PVP, and PVP could penetrate the porcine skin. Here we have also shown that by varying the ratio of HA/PVP, the dissolution rate of the microneedle patches could be control. The needles with higher PVP content possess a higher dissolution rate. These HA/PVP microneedle is potential drug delivery system for various drugs. As a result, we also demonstrate the preparation of retinal-loaded HA/PVP microneedle patches.

REFERENCES

1. Prausnitz, M. R.; Langer, R. J. N. b., Transdermal drug delivery. **2008**, *26* (11), 1261.
2. Wang, M.; Hu, L.; Xu, C., Recent advances in the design of polymeric microneedles for transdermal drug delivery and biosensing. *Lab on a Chip* **2017**, *17* (8), 1373-1387.
3. Chu, L. Y.; Choi, S.-O.; Prausnitz, M. R. J. J. o. p. s., Fabrication of dissolving polymer microneedles for controlled drug encapsulation and delivery: bubble and pedestal microneedle designs. **2010**, *99* (10), 4228-4238.
4. Lee, I.-C.; He, J.-S.; Tsai, M.-T.; Lin, K.-C. J. J. o. M. C. B., Fabrication of a novel partially dissolving polymer microneedle patch for transdermal drug delivery. **2015**, *3* (2), 276-285.
5. Yu, J.; Zhang, Y.; Ye, Y.; DiSanto, R.; Sun, W.; Ranson, D.; Ligler, F. S.; Buse, J. B.; Gu, Z. J. P. o. t. N. A. o. S., Microneedle-array patches loaded with hypoxia-sensitive vesicles provide fast glucose-responsive insulin delivery. **2015**, *112* (27), 8260-8265.
6. Zhu, Z.; Luo, H.; Lu, W.; Luan, H.; Wu, Y.; Luo, J.; Wang, Y.; Pi, J.; Lim, C. Y.; Wang, H. J. P. r., Rapidly dissolvable microneedle patches for transdermal delivery of exenatide. **2014**, *31* (12), 3348-3360.
7. Choi, J.-T.; Park, S.-J.; Park, J.-H. J. J. o. d. t., Microneedles containing cross-linked hyaluronic acid particulates for control of degradation and swelling behaviour after administration into skin. **2018**, 1-11.
8. Lee, J. W.; Park, J.-H.; Prausnitz, M. R. J. B., Dissolving microneedles for transdermal drug delivery. **2008**, *29* (13), 2113-2124.
9. Yang, S.; Feng, Y.; Zhang, L.; Chen, N.; Yuan, W.; Jin, T. J. I. j. o. n., A scalable fabrication process of polymer microneedles. **2012**, *7*, 1415.
10. Wang, Q. L.; Zhu, D. D.; Liu, X. B.; Chen, B. Z.; Guo, X. D. J. S. r., Microneedles with controlled bubble sizes and drug distributions for efficient transdermal drug delivery. **2016**, *6*, 38755.
11. Sullivan, S. P.; Koutsonanos, D. G.; del Pilar Martin, M.; Lee, J. W.; Zarnitsyn, V.; Choi, S.-O.; Murthy, N.; Compans, R. W.; Skountzou, I.; Prausnitz, M. R. J. N. m., Dissolving polymer microneedle patches for influenza vaccination. **2010**, *16* (8), 915.

12. Chen, W.; Wang, C.; Yan, L.; Huang, L.; Zhu, X.; Chen, B.; Sant, H. J.; Niu, X.; Zhu, G.; Yu, K. J. J. o. M. C. B., Improved polyvinylpyrrolidone microneedle arrays with non-stoichiometric cyclodextrin. **2014**, *2* (12), 1699-1705.
13. Lee, I.-C.; Wu, Y.-C.; Tsai, S.-W.; Chen, C.-H.; Wu, M.-H. J. R. A., Fabrication of two-layer dissolving polyvinylpyrrolidone microneedles with different molecular weights for in vivo insulin transdermal delivery. **2017**, *7* (9), 5067-5075.
14. Chen, M.-C.; Lin, Z.-W.; Ling, M.-H. J. A. n., Near-infrared light-activatable microneedle system for treating superficial tumors by combination of chemotherapy and photothermal therapy. **2015**, *10* (1), 93-101.
15. Kim, J. D.; Kim, M.; Yang, H.; Lee, K.; Jung, H. J. J. o. c. r., Droplet-born air blowing: novel dissolving microneedle fabrication. **2013**, *170* (3), 430-436.
16. Lee, K.; Lee, H. C.; Lee, D. S.; Jung, H. J. A. M., Drawing lithography: three-dimensional fabrication of an ultrahigh-aspect-ratio microneedle. **2010**, *22* (4), 483-486.
17. Matteucci, M.; Fanetti, M.; Casella, M.; Gramatica, F.; Gavioli, L.; Tormen, M.; Greci, G.; De Angelis, F.; Di Fabrizio, E. J. M. E., Poly vinyl alcohol re-usable masters for microneedle replication. **2009**, *86* (4-6), 752-756.

VITA

NAME Teeranut Rutwaree

DATE OF BIRTH 2 January 1994

PLACE OF BIRTH Rayong

INSTITUTIONS ATTENDED Bachelor's Degree of Science in Chemistry from
Chulalongkorn University in 2013

HOME ADDRESS 157/10 Village No.2, Phe Sub-district, Muang District,
Rayong 21160



จุฬาลงกรณ์มหาวิทยาลัย
CHULALONGKORN UNIVERSITY